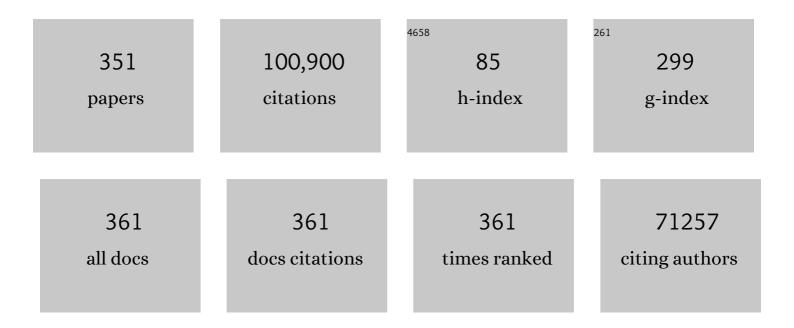
Paul D. Adams

List of Publications by Year in descending order

Source: https://exaly.com/author-pdf/2075970/publications.pdf Version: 2024-02-01



PALLE D ADAMS

#	Article	IF	CITATIONS
1	Integration of software tools for integrative modeling of biomolecular systems. Journal of Structural Biology, 2022, 214, 107841.	2.8	7
2	Modular automated bottom-up proteomic sample preparation for high-throughput applications. PLoS ONE, 2022, 17, e0264467.	2.5	3
3	A Synthetic Gene Library Yields a Previously Unknown Clycoside Phosphorylase That Degrades and Assembles Poly-β-1,3-GlcNAc, Completing the Suite of β-Linked GlcNAc Polysaccharides. ACS Central Science, 2022, 8, 430-440.	11.3	7
4	<i>O</i> -/ <i>N</i> -/ <i>S</i> -Specificity in Glycosyltransferase Catalysis: From Mechanistic Understanding to Engineering. ACS Catalysis, 2021, 11, 1810-1815.	11.2	42
5	Cryo-EM model validation recommendations based on outcomes of the 2019 EMDataResource challenge. Nature Methods, 2021, 18, 156-164.	19.0	73
6	Protein identification from electron cryomicroscopy maps by automated model building and side-chain matching. Acta Crystallographica Section D: Structural Biology, 2021, 77, 457-462.	2.3	9
7	Mechanism Across Scales: A Holistic Modeling Framework Integrating Laboratory and Field Studies for Microbial Ecology. Frontiers in Microbiology, 2021, 12, 642422.	3.5	12
8	Efficient production of oxidized terpenoids via engineering fusion proteins of terpene synthase and cytochrome P450. Metabolic Engineering, 2021, 64, 41-51.	7.0	33
9	Engineering Saccharomyces cerevisiae for isoprenol production. Metabolic Engineering, 2021, 64, 154-166.	7.0	34
10	Experimental and theoretical insights into the effects of pH on catalysis of bond-cleavage by the lignin peroxidase isozyme H8 from Phanerochaete chrysosporium. Biotechnology for Biofuels, 2021, 14, 108.	6.2	10
11	A multiplexed nanostructure-initiator mass spectrometry (NIMS) assay for simultaneously detecting glycosyl hydrolase and lignin modifying enzyme activities. Scientific Reports, 2021, 11, 11803.	3.3	7
12	Reply to Wang et al.: Clear evidence of binding of Ox to the oxygen-evolving complex of photosystem II is best observed in the omit map. Proceedings of the National Academy of Sciences of the United States of America, 2021, 118, e2102342118.	7.1	7
13	Accurate prediction of protein structures and interactions using a three-track neural network. Science, 2021, 373, 871-876.	12.6	2,843
14	Macromolecular refinement of X-ray and cryoelectron microscopy structures with Phenix/OPLS3e for improved structure and ligand quality. Structure, 2021, 29, 913-921.e4.	3.3	29
15	<i>CERES</i> : a cryo-EM re-refinement system for continuous improvement of deposited models. Acta Crystallographica Section D: Structural Biology, 2021, 77, 48-61.	2.3	14
16	Structural dynamics in the water and proton channels of photosystem II during the S2 to S3 transition. Nature Communications, 2021, 12, 6531.	12.8	73
17	Cryoâ€EM map interpretation and protein modelâ€building using iterative map segmentation. Protein Science, 2020, 29, 87-99.	7.6	27
18	Structural Mechanism of Regioselectivity in an Unusual Bacterial Acyl-CoA Dehydrogenase. Journal of the American Chemical Society, 2020, 142, 835-846.	13.7	9

#	Article	IF	CITATIONS
19	Characterization of a Metal-Resistant Bacillus Strain With a High Molybdate Affinity ModA From Contaminated Sediments at the Oak Ridge Reservation. Frontiers in Microbiology, 2020, 11, 587127.	3.5	11
20	Novel bacterial clade reveals origin of form I Rubisco. Nature Plants, 2020, 6, 1158-1166.	9.3	46
21	Improvement of cryo-EM maps by density modification. Nature Methods, 2020, 17, 923-927.	19.0	243
22	Draft Genome Sequence of <i>Bacillus</i> sp. Strain EB106-08-02-XG196, Isolated from High-Nitrate-Contaminated Sediment. Microbiology Resource Announcements, 2020, 9, .	0.6	0
23	A Global Ramachandran Score Identifies Protein Structures with Unlikely Stereochemistry. Structure, 2020, 28, 1249-1258.e2.	3.3	86
24	Implementation of the riding hydrogen model in CCTBX to support the next generation of X-ray and neutron joint refinement in Phenix. Methods in Enzymology, 2020, 634, 177-199.	1.0	8
25	An iron (II) dependent oxygenase performs the last missing step of plant lysine catabolism. Nature Communications, 2020, 11, 2931.	12.8	11
26	Response of <i>Pseudomonas putida</i> to Complex, Aromaticâ€Rich Fractions from Biomass. ChemSusChem, 2020, 13, 4455-4467.	6.8	23
27	What are the current limits on determination of protonation state using neutron macromolecular crystallography?. Methods in Enzymology, 2020, 634, 225-255.	1.0	0
28	Structure and Function of BorB, the Type II Thioesterase from the Borrelidin Biosynthetic Gene Cluster. Biochemistry, 2020, 59, 1630-1639.	2.5	10
29	Untangling the sequence of events during the S ₂ → S ₃ transition in photosystem II and implications for the water oxidation mechanism. Proceedings of the National Academy of Sciences of the United States of America, 2020, 117, 12624-12635.	7.1	149
30	Improved chemistry restraints for crystallographic refinement by integrating the Amber force field into <i>Phenix</i> . Acta Crystallographica Section D: Structural Biology, 2020, 76, 51-62.	2.3	29
31	Density modification of cryo-EM maps. Acta Crystallographica Section D: Structural Biology, 2020, 76, 912-925.	2.3	28
32	Arginine off-kilter: guanidinium is not as planar as restraints denote. Acta Crystallographica Section D: Structural Biology, 2020, 76, 1159-1166.	2.3	7
33	Cryo_fit: Democratization of flexible fitting for cryo-EM. Journal of Structural Biology, 2019, 208, 1-6.	2.8	30
34	Automated "Cells-To-Peptides―Sample Preparation Workflow for High-Throughput, Quantitative Proteomic Assays of Microbes. Journal of Proteome Research, 2019, 18, 3752-3761.	3.7	32
35	Optimization of the IPP-bypass mevalonate pathway and fed-batch fermentation for the production of isoprenol in Escherichia coli. Metabolic Engineering, 2019, 56, 85-96.	7.0	46
36	Structural insights into dehydratase substrate selection for the borrelidin and fluvirucin polyketide synthases. Journal of Industrial Microbiology and Biotechnology, 2019, 46, 1225-1235.	3.0	7

#	Article	IF	CITATIONS
37	Massively Parallel Fitness Profiling Reveals Multiple Novel Enzymes in <i>Pseudomonas putida</i> Lysine Metabolism. MBio, 2019, 10, .	4.1	60
38	Methyl ketone production by <i>Pseudomonas putida</i> is enhanced by plantâ€derived amino acids. Biotechnology and Bioengineering, 2019, 116, 1909-1922.	3.3	29
39	A rapid methods development workflow for high-throughput quantitative proteomic applications. PLoS ONE, 2019, 14, e0211582.	2.5	17
40	Announcing mandatory submission of PDBx/mmCIF format files for crystallographic depositions to the Protein Data Bank (PDB). Acta Crystallographica Section D: Structural Biology, 2019, 75, 451-454.	2.3	46
41	Iron―and aluminium―nduced depletion of molybdenum in acidic environments impedes the nitrogen cycle. Environmental Microbiology, 2019, 21, 152-163.	3.8	22
42	Iron–sulfur clusters have no right angles. Acta Crystallographica Section D: Structural Biology, 2019, 75, 16-20.	2.3	16
43	Macromolecular structure determination using X-rays, neutrons and electrons: recent developments in <i>Phenix</i> . Acta Crystallographica Section D: Structural Biology, 2019, 75, 861-877.	2.3	4,060
44	Updated validation and deposition tools in the <i>Phenix</i> GUI. Acta Crystallographica Section A: Foundations and Advances, 2019, 75, a339-a339.	0.1	0
45	Developing a shared computing and networking infrastructure for the ALS-ENABLE structural biology program at the Advanced Light Source. Acta Crystallographica Section A: Foundations and Advances, 2019, 75, a248-a248.	0.1	0
46	Efficient real-space refinement for cryo-EM and crystallography. Acta Crystallographica Section A: Foundations and Advances, 2019, 75, e86-e86.	0.1	0
47	Microbial Functional Gene Diversity Predicts Groundwater Contamination and Ecosystem Functioning. MBio, 2018, 9, .	4.1	57
48	Integrated analysis of isopentenyl pyrophosphate (IPP) toxicity in isoprenoid-producing Escherichia coli. Metabolic Engineering, 2018, 47, 60-72.	7.0	106
49	Toward industrial production of isoprenoids in <i>Escherichia coli</i> : Lessons learned from CRISPRâ€Cas9 based optimization of a chromosomally integrated mevalonate pathway. Biotechnology and Bioengineering, 2018, 115, 1000-1013.	3.3	39
50	Employing a biochemical protecting group for a sustainable indigo dyeing strategy. Nature Chemical Biology, 2018, 14, 256-261.	8.0	143
51	<i>DiSCaMB</i> : a software library for aspherical atom model X-ray scattering factor calculations with CPUs and GPUs. Journal of Applied Crystallography, 2018, 51, 193-199.	4.5	24
52	Discovery of enzymes for toluene synthesis from anoxic microbial communities. Nature Chemical Biology, 2018, 14, 451-457.	8.0	47
53	Interactive comparison and remediation of collections of macromolecular structures. Protein Science, 2018, 27, 182-194.	7.6	13
54	MolProbity: More and better reference data for improved allâ€atom structure validation. Protein Science, 2018, 27, 293-315.	7.6	2,776

#	Article	IF	CITATIONS
55	A bacterial pioneer produces cellulase complexes that persist through community succession. Nature Microbiology, 2018, 3, 99-107.	13.3	38
56	Structures of the intermediates of Kok's photosynthetic water oxidation clock. Nature, 2018, 563, 421-425.	27.8	386
57	Distribution of evaluation scores for the models submitted to the second cryo-EM model challenge. Data in Brief, 2018, 20, 1629-1638.	1.0	5
58	Rapid characterization of the activities of lignin-modifying enzymes based on nanostructure-initiator mass spectrometry (NIMS). Biotechnology for Biofuels, 2018, 11, 266.	6.2	14
59	Renewable production of high density jet fuel precursor sesquiterpenes from Escherichia coli. Biotechnology for Biofuels, 2018, 11, 285.	6.2	43
60	Engineering glycoside hydrolase stability by the introduction of zinc binding. Acta Crystallographica Section D: Structural Biology, 2018, 74, 702-710.	2.3	1
61	A fully automatic method yielding initial models from high-resolution cryo-electron microscopy maps. Nature Methods, 2018, 15, 905-908.	19.0	137
62	Jungle Express is a versatile repressor system for tight transcriptional control. Nature Communications, 2018, 9, 3617.	12.8	33
63	Automated flow-based/digital microfluidic platform integrated with onsite electroporation process for multiplex genetic engineering applications. , 2018, , .		5
64	Map segmentation, automated model-building and their application to the Cryo-EM Model Challenge. Journal of Structural Biology, 2018, 204, 338-343.	2.8	6
65	Evaluation system and web infrastructure for the second cryo-EM model challenge. Journal of Structural Biology, 2018, 204, 96-108.	2.8	11
66	From deep TLS validation to ensembles of atomic models built from elemental motions. II. Analysis of TLS refinement results by explicit interpretation. Acta Crystallographica Section D: Structural Biology, 2018, 74, 621-631.	2.3	7
67	Improved chemistry restraints for crystallographic refinement by integrating Amber molecular mechanics in Phenix. Acta Crystallographica Section A: Foundations and Advances, 2018, 74, a145-a145.	0.1	2
68	Evaluation of models determined by neutron diffraction and proposed improvements to their validation and deposition. Acta Crystallographica Section D: Structural Biology, 2018, 74, 800-813.	2.3	15
69	Automated map sharpening by maximization of detail and connectivity. Acta Crystallographica Section D: Structural Biology, 2018, 74, 545-559.	2.3	218
70	Real-space refinement in <i>PHENIX</i> for cryo-EM and crystallography. Acta Crystallographica Section D: Structural Biology, 2018, 74, 531-544.	2.3	2,065
71	New tools for the analysis and validation of cryo-EM maps and atomic models. Acta Crystallographica Section D: Structural Biology, 2018, 74, 814-840.	2.3	575
72	Polder maps: improving OMIT maps for ligand building and validation. Acta Crystallographica Section A: Foundations and Advances, 2018, 74, a308-a308.	0.1	0

#	Article	IF	CITATIONS
73	The collaborative crystallography program at the Advanced Light Source. Acta Crystallographica Section A: Foundations and Advances, 2018, 74, a431-a431.	0.1	0
74	High-throughput protein–ligand complex structure solution with Phenix. Acta Crystallographica Section A: Foundations and Advances, 2018, 74, a445-a445.	0.1	0
75	Self-assembled gold nanoparticle film for nanostructure-initiator mass spectrometry with passive on-line salt fractionation. , 2017, , .		0
76	Parallel microarraying of microfluidic droplets for high-throughput integration with matrix-assisted laser desorption ionization mass spectrometry. , 2017, , .		0
77	Accurate model annotation of a near-atomic resolution cryo-EM map. Proceedings of the National Academy of Sciences of the United States of America, 2017, 114, 3103-3108.	7.1	111
78	Structure of the human TRiC/CCT Subunit 5 associated with hereditary sensory neuropathy. Scientific Reports, 2017, 7, 3673.	3.3	31
79	Structure of aryl O-demethylase offers molecular insight into a catalytic tyrosine-dependent mechanism. Proceedings of the National Academy of Sciences of the United States of America, 2017, 114, E3205-E3214.	7.1	24
80	Production of jet fuel precursor monoterpenoids from engineered <i>Escherichia coli</i> . Biotechnology and Bioengineering, 2017, 114, 1703-1712.	3.3	81
81	On-chip integration of droplet microfluidics and nanostructure-initiator mass spectrometry for enzyme screening. Lab on A Chip, 2017, 17, 323-331.	6.0	44
82	The Experiment Data Depot: A Web-Based Software Tool for Biological Experimental Data Storage, Sharing, and Visualization. ACS Synthetic Biology, 2017, 6, 2248-2259.	3.8	45
83	The cryo-electron microscopy structure of human transcription factor IIH. Nature, 2017, 549, 414-417.	27.8	89
84	Comprehensive <i>in Vitro</i> Analysis of Acyltransferase Domain Exchanges in Modular Polyketide Synthases and Its Application for Short-Chain Ketone Production. ACS Synthetic Biology, 2017, 6, 139-147.	3.8	100
85	Polder maps: improving OMIT maps for ligand building and validation. Acta Crystallographica Section A: Foundations and Advances, 2017, 73, C48-C48.	0.1	0
86	Polder maps: improving OMIT maps by excluding bulk solvent. Acta Crystallographica Section D: Structural Biology, 2017, 73, 148-157.	2.3	500
87	Reply to Kiser: Dioxygen binding in NOV1 crystal structures. Proceedings of the National Academy of Sciences of the United States of America, 2017, 114, E6029-E6030.	7.1	4
88	Plant cell wall glycosyltransferases: High-throughput recombinant expression screening and general requirements for these challenging enzymes. PLoS ONE, 2017, 12, e0177591.	2.5	21
89	Expression of naturally ionic liquid-tolerant thermophilic cellulases in Aspergillus niger. PLoS ONE, 2017, 12, e0189604.	2.5	13
90	X-ray diffraction analysis and <i>in vitro</i> characterization of the UAM2 protein from <i>Oryza sativa</i> . Acta Crystallographica Section F, Structural Biology Communications, 2017, 73, 241-245.	0.8	1

#	Article	IF	CITATIONS
91	Berkeley Screen: a set of 96 solutions for general macromolecular crystallization. Journal of Applied Crystallography, 2017, 50, 1352-1358.	4.5	11
92	An editor for the generation and customization of geometry restraints. Acta Crystallographica Section D: Structural Biology, 2017, 73, 123-130.	2.3	27
93	Phasing strategies II – molecular replacement. Acta Crystallographica Section A: Foundations and Advances, 2017, 73, a391-a391.	0.1	0
94	Model-building using cryo-EM and crystallographic maps. Acta Crystallographica Section A: Foundations and Advances, 2017, 73, C1327-C1327.	0.1	0
95	Video tutorials for the <i>Phenix</i> software suite. Acta Crystallographica Section A: Foundations and Advances, 2017, 73, C1134-C1134.	0.1	0
96	Structure and mechanism of NOV1, a resveratrol-cleaving dioxygenase. Proceedings of the National Academy of Sciences of the United States of America, 2016, 113, 14324-14329.	7.1	50
97	Can I solve my structure by SAD phasing? Planning an experiment, scaling data and evaluating the useful anomalous correlation and anomalous signal. Acta Crystallographica Section D: Structural Biology, 2016, 72, 359-374.	2.3	29
98	No observable conformational changes in PSII. Nature, 2016, 533, E1-E2.	27.8	40
99	Nonâ€invasive imaging of cellulose microfibril orientation within plant cell walls by polarized Raman microspectroscopy. Biotechnology and Bioengineering, 2016, 113, 82-90.	3.3	21
100	Structural and Biochemical Characterization of the Early and Late Enzymes in the Lignin β-Aryl Ether Cleavage Pathway from Sphingobium sp. SYK-6. Journal of Biological Chemistry, 2016, 291, 10228-10238.	3.4	44
101	Characterizing Strain Variation in Engineered E.Âcoli Using a Multi-Omics-Based Workflow. Cell Systems, 2016, 2, 335-346.	6.2	73
102	Comparative Community Proteomics Demonstrates the Unexpected Importance of Actinobacterial Glycoside Hydrolase Family 12 Protein for Crystalline Cellulose Hydrolysis. MBio, 2016, 7, .	4.1	17
103	Structure of photosystem II and substrate binding at room temperature. Nature, 2016, 540, 453-457.	27.8	323
104	Can I solve my structure by SAD phasing? Anomalous signal in SAD phasing. Acta Crystallographica Section D: Structural Biology, 2016, 72, 346-358.	2.3	31
105	A second-generation expression system for tyrosine-sulfated proteins and its application in crop protection. Integrative Biology (United Kingdom), 2016, 8, 542-545.	1.3	23
106	A Droplet Microfluidic Platform for Automating Genetic Engineering. ACS Synthetic Biology, 2016, 5, 426-433.	3.8	63
107	Exploiting the Substrate Promiscuity of Hydroxycinnamoyl-CoA:Shikimate Hydroxycinnamoyl Transferase to Reduce Lignin. Plant and Cell Physiology, 2016, 57, 568-579.	3.1	78
108	Structural Basis of Stereospecificity in the Bacterial Enzymatic Cleavage of β-Aryl Ether Bonds in Lignin. Journal of Biological Chemistry, 2016, 291, 5234-5246.	3.4	40

#	Article	IF	CITATIONS
109	A new default restraint library for the protein backbone in <i>Phenix</i> : a conformation-dependent geometry goes mainstream. Acta Crystallographica Section D: Structural Biology, 2016, 72, 176-179.	2.3	39
110	Improved ligand geometries in crystallographic refinement using <i>AFITT</i> in <i>PHENIX</i> . Acta Crystallographica Section D: Structural Biology, 2016, 72, 1062-1072.	2.3	29
111	New bulk-solvent model improves model-to-data fit and facilitates map interpretation. Acta Crystallographica Section A: Foundations and Advances, 2016, 72, s22-s22.	0.1	Ο
112	Predicting X-ray diffuse scattering from translation–libration–screw structural ensembles. Acta Crystallographica Section D: Biological Crystallography, 2015, 71, 1657-1667.	2.5	14
113	Analytics for Metabolic Engineering. Frontiers in Bioengineering and Biotechnology, 2015, 3, 135.	4.1	79
114	Development of a High Throughput Platform for Screening Glycoside Hydrolases Based on Oxime-NIMS. Frontiers in Bioengineering and Biotechnology, 2015, 3, 153.	4.1	14
115	Use of Nanostructure-Initiator Mass Spectrometry to Deduce Selectivity of Reaction in Glycoside Hydrolases. Frontiers in Bioengineering and Biotechnology, 2015, 3, 165.	4.1	6
116	Natural Bacterial Communities Serve as Quantitative Geochemical Biosensors. MBio, 2015, 6, e00326-15.	4.1	173
117	The Berkeley Center for Structural Biology at the Advanced Light Source. Synchrotron Radiation News, 2015, 28, 22-27.	0.8	2
118	NMR Exchange Format: a unified and open standard for representation of NMR restraint data. Nature Structural and Molecular Biology, 2015, 22, 433-434.	8.2	40
119	Multifunctional cellulase catalysis targeted by fusion to different carbohydrate-binding modules. Biotechnology for Biofuels, 2015, 8, 220.	6.2	49
120	Programming new geometry restraints: parallelity of atomic groups. Journal of Applied Crystallography, 2015, 48, 1130-1141.	4.5	13
121	Principal component analysis of proteomics (PCAP) as a tool to direct metabolic engineering. Metabolic Engineering, 2015, 28, 123-133.	7.0	140
122	Metabolic engineering for the high-yield production of isoprenoid-based C5 alcohols in E. coli. Scientific Reports, 2015, 5, 11128.	3.3	125
123	Identification and Characterization of a Golgi-Localized UDP-Xylose Transporter Family from Arabidopsis. Plant Cell, 2015, 27, 1218-1227.	6.6	61
124	FEM: feature-enhanced map. Acta Crystallographica Section D: Biological Crystallography, 2015, 71, 646-666.	2.5	157
125	A Versatile Microfluidic Device for Automating Synthetic Biology. ACS Synthetic Biology, 2015, 4, 1151-1164.	3.8	81
126	Outcome of the First wwPDB Hybrid/Integrative Methods Task Force Workshop. Structure, 2015, 23, 1156-1167.	3.3	159

8

#	Article	IF	CITATIONS
127	Indexing amyloid peptide diffraction from serial femtosecond crystallography: new algorithms for sparse patterns. Acta Crystallographica Section D: Biological Crystallography, 2015, 71, 357-366.	2.5	18
128	Using support vector machines to improve elemental ion identification in macromolecular crystal structures. Acta Crystallographica Section D: Biological Crystallography, 2015, 71, 1147-1158.	2.5	4
129	Standard Flow Liquid Chromatography for Shotgun Proteomics in Bioenergy Research. Frontiers in Bioengineering and Biotechnology, 2015, 3, 44.	4.1	44
130	EMRinger: side chain–directed model and map validation for 3D cryo-electron microscopy. Nature Methods, 2015, 12, 943-946.	19.0	799
131	Macromolecular X-ray structure determination using weak, single-wavelength anomalous data. Nature Methods, 2015, 12, 127-130.	19.0	31
132	A droplet-to-digital (D2D) microfluidic device for single cell assays. Lab on A Chip, 2015, 15, 225-236.	6.0	70
133	From deep TLS validation to ensembles of atomic models built from elemental motions. Acta Crystallographica Section D: Biological Crystallography, 2015, 71, 1668-1683.	2.5	14
134	Macromolecular crystallographic estructure refinement. Arbor, 2015, 191, a219.	0.3	3
135	Cellulosic Biomass Pretreatment and Sugar Yields as a Function of Biomass Particle Size. PLoS ONE, 2014, 9, e100836.	2.5	19
136	Development of a Native Escherichia coli Induction System for Ionic Liquid Tolerance. PLoS ONE, 2014, 9, e101115.	2.5	31
137	Understanding the Role of Histidine in the GHSxG Acyltransferase Active Site Motif: Evidence for Histidine Stabilization of the Malonyl-Enzyme Intermediate. PLoS ONE, 2014, 9, e109421.	2.5	10
138	Pressure stabilizer for reproducible picoinjection in droplet microfluidic systems. Lab on A Chip, 2014, 14, 4533-4539.	6.0	34
139	A Peptide-Based Method for 13C Metabolic Flux Analysis in Microbial Communities. PLoS Computational Biology, 2014, 10, e1003827.	3.2	56
140	An atomic model of brome mosaic virus using direct electron detection and real-space optimization. Nature Communications, 2014, 5, 4808.	12.8	105
141	Structural and Biochemical Studies of Actin in Complex with Synthetic Macrolide Tail Analogues. ChemMedChem, 2014, 9, 2286-2293.	3.2	20
142	Conformationâ€dependent backbone geometry restraints set a new standard for protein crystallographic refinement. FEBS Journal, 2014, 281, 4061-4071.	4.7	36
143	Conformational dynamics of a crystalline protein from microsecond-scale molecular dynamics simulations and diffuse X-ray scattering. Proceedings of the National Academy of Sciences of the United States of America, 2014, 111, 17887-17892.	7.1	55
144	Error Rate Comparison during Polymerase Chain Reaction by DNA Polymerase. Molecular Biology International, 2014, 2014, 1-8.	1.7	160

#	Article	IF	CITATIONS
145	Improved crystal orientation and physical properties from single-shot XFEL stills. Acta Crystallographica Section D: Biological Crystallography, 2014, 70, 3299-3309.	2.5	38
146	Metrics for comparison of crystallographic maps. Acta Crystallographica Section D: Biological Crystallography, 2014, 70, 2593-2606.	2.5	29
147	Structure of the OsSERK2 leucine-rich repeat extracellular domain. Acta Crystallographica Section D: Biological Crystallography, 2014, 70, 3080-3086.	2.5	16
148	Accurate macromolecular structures using minimal measurements from X-ray free-electron lasers. Nature Methods, 2014, 11, 545-548.	19.0	140
149	Correlation analysis of targeted proteins and metabolites to assess and engineer microbial isopentenol production. Biotechnology and Bioengineering, 2014, 111, 1648-1658.	3.3	89
150	Rapid Kinetic Characterization of Glycosyl Hydrolases Based on Oxime Derivatization and Nanostructure-Initiator Mass Spectrometry (NIMS). ACS Chemical Biology, 2014, 9, 1470-1479.	3.4	36
151	CRYO-EM Atomic Model of Brome Mosaic Virus Derived from Direct Electron Detection Images and a Real-Space Model Optimization Protocol. Biophysical Journal, 2014, 106, 600a.	0.5	2
152	Analysis of plant nucleotide sugars by hydrophilic interaction liquid chromatography and tandem mass spectrometry. Analytical Biochemistry, 2014, 448, 14-22.	2.4	49
153	Production of anteiso-branched fatty acids in Escherichia coli; next generation biofuels with improved cold-flow properties. Metabolic Engineering, 2014, 26, 111-118.	7.0	55
154	<i>In Vitro</i> Analysis of Carboxyacyl Substrate Tolerance in the Loading and First Extension Modules of Borrelidin Polyketide Synthase. Biochemistry, 2014, 53, 5975-5977.	2.5	21
155	Identification of a Sphingolipid α-Glucuronosyltransferase That Is Essential for Pollen Function in <i>Arabidopsis</i> Â Â Â. Plant Cell, 2014, 26, 3314-3325.	6.6	80
156	Automated identification of elemental ions in macromolecular crystal structures. Acta Crystallographica Section D: Biological Crystallography, 2014, 70, 1104-1114.	2.5	40
157	Phylogenomically Guided Identification of Industrially Relevant GH1 β-Glucosidases through DNA Synthesis and Nanostructure-Initiator Mass Spectrometry. ACS Chemical Biology, 2014, 9, 2082-2091.	3.4	78
158	Constructing Tailored Isoprenoid Products by Structure-Guided Modification of Geranylgeranyl Reductase. Structure, 2014, 22, 1028-1036.	3.3	28
159	A targeted proteomics toolkit for high-throughput absolute quantification of Escherichia coli proteins. Metabolic Engineering, 2014, 26, 48-56.	7.0	45
160	Taking snapshots of photosynthetic water oxidation using femtosecond X-ray diffraction and spectroscopy. Nature Communications, 2014, 5, 4371.	12.8	206
161	Biochemical and Structural Studies of NADH-Dependent FabG Used To Increase the Bacterial Production of Fatty Acids under Anaerobic Conditions. Applied and Environmental Microbiology, 2014, 80, 497-505.	3.1	42
162	Combining Crystallographic and Structure-Modeling Approaches in Macromolecular Crystallography. Biophysical Journal, 2014, 106, 34a.	0.5	0

#	Article	IF	CITATIONS
163	The plant glycosyltransferase clone collection for functional genomics. Plant Journal, 2014, 79, 517-529.	5.7	67
164	Diffuse X-Ray Scattering for Ensemble Modeling of Crystalline Proteins. Biophysical Journal, 2014, 106, 384a.	0.5	0
165	Automating crystallographic structure solution and refinement of protein–ligand complexes. Acta Crystallographica Section D: Biological Crystallography, 2014, 70, 144-154.	2.5	43
166	Ligand placement based on prior structures: the guided ligand-replacement method. Acta Crystallographica Section D: Biological Crystallography, 2014, 70, 134-143.	2.5	11
167	Flexible torsion-angle noncrystallographic symmetry restraints for improved macromolecular structure refinement. Acta Crystallographica Section D: Biological Crystallography, 2014, 70, 1346-1356.	2.5	19
168	Addition of a carbohydrate-binding module enhances cellulase penetration into cellulose substrates. Biotechnology for Biofuels, 2013, 6, 93.	6.2	63
169	Application of targeted proteomics and biological parts assembly in E. coli to optimize the biosynthesis of an anti-malarial drug precursor, amorpha-4,11-diene. Chemical Engineering Science, 2013, 103, 21-28.	3.8	14
170	Understanding the impact of ionic liquid pretreatment on cellulose and lignin via thermochemical analysis. Biomass and Bioenergy, 2013, 54, 276-283.	5.7	55
171	Metabolic engineering of Escherichia coli for limonene and perillyl alcohol production. Metabolic Engineering, 2013, 19, 33-41.	7.0	343
172	Engineering dynamic pathway regulation using stress-response promoters. Nature Biotechnology, 2013, 31, 1039-1046.	17.5	411
173	<i>TLS</i> from fundamentals to practice. Crystallography Reviews, 2013, 19, 230-270.	1.5	46
174	A universal flow cytometry assay for screening carbohydrate-active enzymes using glycan microspheres. Chemical Communications, 2013, 49, 5441.	4.1	5
175	Improved low-resolution crystallographic refinement with Phenix and Rosetta. Nature Methods, 2013, 10, 1102-1104.	19.0	175
176	Improved Crystallographic Structures Using Extensive Combinatorial Refinement. Structure, 2013, 21, 1923-1930.	3.3	18
177	Simultaneous Femtosecond X-ray Spectroscopy and Diffraction of Photosystem II at Room Temperature. Science, 2013, 340, 491-495.	12.6	378
178	Utilizing a highly responsive gene, yhjX, in E. coli based production of 1,4-butanediol. Chemical Engineering Science, 2013, 103, 68-73.	3.8	13
179	Advances, Interactions, and Future Developments in the CNS, Phenix, and Rosetta Structural Biology Software Systems. Annual Review of Biophysics, 2013, 42, 265-287.	10.0	88
180	Survey of renewable chemicals produced from lignocellulosic biomass during ionic liquid pretreatment. Biotechnology for Biofuels, 2013, 6, 14.	6.2	151

#	Article	IF	CITATIONS
181	Droplet-based microfluidic platform for heterogeneous enzymatic assays. Lab on A Chip, 2013, 13, 1817.	6.0	42
182	Three Novel Rice Genes Closely Related to the ArabidopsisIRX9, IRX9L, and IRX14 Genes and Their Roles in Xylan Biosynthesis. Frontiers in Plant Science, 2013, 4, 83.	3.6	83
183	From Soil to Structure, a Novel Dimeric β-Glucosidase Belonging to Glycoside Hydrolase Family 3 Isolated from Compost Using Metagenomic Analysis. Journal of Biological Chemistry, 2013, 288, 14985-14992.	3.4	42
184	High throughput nanostructure-initiator mass spectrometry screening of microbial growth conditions for maximal Î ² -glucosidase production. Frontiers in Microbiology, 2013, 4, 365.	3.5	11
185	Intensity statistics in the presence of translational noncrystallographic symmetry. Acta Crystallographica Section D: Biological Crystallography, 2013, 69, 176-183.	2.5	43
186	Bulk-solvent and overall scaling revisited: faster calculations, improved results. Acta Crystallographica Section D: Biological Crystallography, 2013, 69, 625-634.	2.5	79
187	Model morphing and sequence assignment after molecular replacement. Acta Crystallographica Section D: Biological Crystallography, 2013, 69, 2244-2250.	2.5	37
188	<i>Phaser.MRage</i> : automated molecular replacement. Acta Crystallographica Section D: Biological Crystallography, 2013, 69, 2276-2286.	2.5	216
189	Validated near-atomic resolution structure of bacteriophage epsilon15 derived from cryo-EM and modeling. Proceedings of the National Academy of Sciences of the United States of America, 2013, 110, 12301-12306.	7.1	68
190	Improved Activity of a Thermophilic Cellulase, Cel5A, from Thermotoga maritima on Ionic Liquid Pretreated Switchgrass. PLoS ONE, 2013, 8, e79725.	2.5	20
191	Golgi Enrichment and Proteomic Analysis of Developing Pinus radiata Xylem by Free-Flow Electrophoresis. PLoS ONE, 2013, 8, e84669.	2.5	11
192	Mechanism of nucleotide sensing in group II chaperonins. EMBO Journal, 2012, 31, 3949-3950.	7.8	2
193	Mechanism of nucleotide sensing in group II chaperonins. EMBO Journal, 2012, 31, 731-740.	7.8	32
194	Supplementation of Intracellular XylR Leads to Coutilization of Hemicellulose Sugars. Applied and Environmental Microbiology, 2012, 78, 2221-2229.	3.1	27
195	Mechanical Stress Analysis as a Method to Understand the Impact of Genetically Engineered Rice and Arabidopsis Plants. Industrial Biotechnology, 2012, 8, 238-244.	0.8	6
196	Shining Light into Black Boxes. Science, 2012, 336, 159-160.	12.6	154
197	Energy-dispersive X-ray emission spectroscopy using an X-ray free-electron laser in a shot-by-shot mode. Proceedings of the National Academy of Sciences of the United States of America, 2012, 109, 19103-19107.	7.1	113
198	Tracing Determinants of Dual Substrate Specificity in Glycoside Hydrolase Family 5. Journal of Biological Chemistry, 2012, 287, 25335-25343.	3.4	39

#	Article	IF	CITATIONS
199	Nanoflow electrospinning serial femtosecond crystallography. Acta Crystallographica Section D: Biological Crystallography, 2012, 68, 1584-1587.	2.5	167
200	Enhancing fatty acid production by the expression of the regulatory transcription factor FadR. Metabolic Engineering, 2012, 14, 653-660.	7.0	173
201	Glycoside Hydrolases from a targeted Compost Metagenome, activity-screening and functional characterization. BMC Biotechnology, 2012, 12, 38.	3.3	48
202	Manipulation of the carbon storage regulator system for metabolite remodeling and biofuel production in Escherichia coli. Microbial Cell Factories, 2012, 11, 79.	4.0	53
203	Automatic Fortran to C++ conversion with FABLE. Source Code for Biology and Medicine, 2012, 7, 5.	1.7	15
204	Thermoascus aurantiacus is a promising source of enzymes for biomass deconstruction under thermophilic conditions. Biotechnology for Biofuels, 2012, 5, 54.	6.2	88
205	Structure of FabH and factors affecting the distribution of branched fatty acids in <i>Micrococcus luteus</i> . Acta Crystallographica Section D: Biological Crystallography, 2012, 68, 1320-1328.	2.5	9
206	Understanding changes in lignin of Panicum virgatum and Eucalyptus globulus as a function of ionic liquid pretreatment. Bioresource Technology, 2012, 126, 156-161.	9.6	60
207	1.7 Refinement of X-ray Crystal Structures. , 2012, , 105-115.		3
208	Encoding substrates with mass tags to resolve stereospecific reactions using Nimzyme. Rapid Communications in Mass Spectrometry, 2012, 26, 611-615.	1.5	20
209	Application of targeted proteomics to metabolically engineered <i><scp>E</scp>scherichia coli</i> . Proteomics, 2012, 12, 1289-1299.	2.2	21
210	Improving the Accuracy of Macromolecular Structure Refinement at 7ÂÃ Resolution. Structure, 2012, 20, 957-966.	3.3	37
211	Room temperature femtosecond X-ray diffraction of photosystem II microcrystals. Proceedings of the National Academy of Sciences of the United States of America, 2012, 109, 9721-9726.	7.1	144
212	The Protein Structure Initiative Structural Biology Knowledgebase Technology Portal: a structural biology web resource. Journal of Structural and Functional Genomics, 2012, 13, 57-62.	1.2	20
213	phenix.mr_rosetta: molecular replacement and model rebuilding with Phenix and Rosetta. Journal of Structural and Functional Genomics, 2012, 13, 81-90.	1.2	131
214	Acoustic deposition with NIMS as a high-throughput enzyme activity assay. Analytical and Bioanalytical Chemistry, 2012, 403, 707-711.	3.7	33
215	Graphical tools for macromolecular crystallography in <i>PHENIX</i> . Journal of Applied Crystallography, 2012, 45, 581-586.	4.5	139
216	Use of knowledge-based restraints in <i>phenix.refine</i> to improve macromolecular refinement at low resolution. Acta Crystallographica Section D: Biological Crystallography, 2012, 68, 381-390.	2.5	230

#	Article	IF	CITATIONS
217	Application of DEN refinement and automated model building to a difficult case of molecular-replacement phasing: the structure of a putative succinyl-diaminopimelate desuccinylase from <i>Corynebacterium glutamicum</i> . Acta Crystallographica Section D: Biological Crystallography, 2012, 68, 391-403.	2.5	26
218	Towards automated crystallographic structure refinement with <i>phenix.refine</i> . Acta Crystallographica Section D: Biological Crystallography, 2012, 68, 352-367.	2.5	4,573
219	Improved crystallographic models through iterated local density-guided model deformation and reciprocal-space refinement. Acta Crystallographica Section D: Biological Crystallography, 2012, 68, 861-870.	2.5	37
220	Raman-spectroscopy-based noninvasive microanalysis of native lignin structure. Analytical and Bioanalytical Chemistry, 2012, 402, 983-987.	3.7	22
221	Molecular replacement and model-building using distant homology models as templates. Acta Crystallographica Section A: Foundations and Advances, 2012, 68, s17-s18.	0.3	1
222	Modelling dynamics in protein crystal structures by ensemble refinement. ELife, 2012, 1, e00311.	6.0	248
223	Colloid-based multiplexed screening for plant biomass-degrading glycoside hydrolase activities in microbial communities. Energy and Environmental Science, 2011, 4, 2884.	30.8	29
224	The Structural Biology Knowledgebase - search Online for Protein Sequences, Structures, Functions, Methods and More. Biophysical Journal, 2011, 100, 319a.	0.5	0
225	Impact of ionic liquid pretreated plant biomass on Saccharomyces cerevisiae growth and biofuel production. Green Chemistry, 2011, 13, 2743.	9.0	139
226	Blind image analysis for the compositional and structural characterization of plant cell walls. Analytica Chimica Acta, 2011, 702, 172-177.	5.4	26
227	The Phenix software for automated determination of macromolecular structures. Methods, 2011, 55, 94-106.	3.8	764
228	A New Generation of Crystallographic Validation Tools for the Protein Data Bank. Structure, 2011, 19, 1395-1412.	3.3	405
229	Structure of a Three-Domain Sesquiterpene Synthase: A Prospective Target for Advanced Biofuels Production. Structure, 2011, 19, 1876-1884.	3.3	76
230	The Structural Biology Knowledgebase: a portal to protein structures, sequences, functions, and methods. Journal of Structural and Functional Genomics, 2011, 12, 45-54.	1.2	65
231	<i>iotbx.cif</i> : a comprehensive CIF toolbox. Journal of Applied Crystallography, 2011, 44, 1259-1263.	4.5	487
232	Exact direct-space asymmetric units for the 230 crystallographic space groups. Acta Crystallographica Section A: Foundations and Advances, 2011, 67, 269-275.	0.3	11
233	High-throughput enzymatic hydrolysis of lignocellulosic biomass via in-situ regeneration. Bioresource Technology, 2011, 102, 1329-1337.	9.6	26
234	Targeted proteomics for metabolic pathway optimization: Application to terpene production. Metabolic Engineering, 2011, 13, 194-203.	7.0	169

#	Article	IF	CITATIONS
235	The Structural Biology Knowledgebase – structures, functions, methods and more. Acta Crystallographica Section A: Foundations and Advances, 2011, 67, C555-C555.	0.3	0
236	Graphical tools for structure determination and refinement inPHENIX. Acta Crystallographica Section A: Foundations and Advances, 2011, 67, C161-C162.	0.3	0
237	Ensemble refinement of protein crystal structures in <i>PHENIX</i> . Acta Crystallographica Section A: Foundations and Advances, 2011, 67, C133-C134.	0.3	1
238	A trigonometric minimum model for refinement. Acta Crystallographica Section A: Foundations and Advances, 2011, 67, C597-C597.	0.3	0
239	Supramolecular Self-Assembled Chaos: Polyphenolic Lignin's Barrier to Cost-Effective Lignocellulosic Biofuels. Molecules, 2010, 15, 8641-8688.	3.8	151
240	Crystal structure of the transcriptional activator HlyU from <i>Vibrio vulnificus</i> CMCP6. FEBS Letters, 2010, 584, 1097-1102.	2.8	18
241	Molecular simulations provide new insights into the role of the accessory immunoglobulinâ€ike domain of Cel9A. FEBS Letters, 2010, 584, 3431-3435.	2.8	17
242	Corrigendum to "Molecular simulations provide new insights into the role of the accessory immunoglobulin-like domain of Cel9A―[FEBS Lett. 584 (2010) 3432-3436]. FEBS Letters, 2010, 584, 3672-3672.	2.8	0
243	<i>phenix.model_vs_data</i> : a high-level tool for the calculation of crystallographic model and data statistics. Journal of Applied Crystallography, 2010, 43, 669-676.	4.5	112
244	<i>PHENIX</i> : a comprehensive Python-based system for macromolecular structure solution. Acta Crystallographica Section D: Biological Crystallography, 2010, 66, 213-221.	2.5	20,564
245	Joint X-ray and neutron refinement with <i>phenix.refine</i> . Acta Crystallographica Section D: Biological Crystallography, 2010, 66, 1153-1163.	2.5	259
246	Opportunities and challenges with the growth of neutron crystallography. Acta Crystallographica Section D: Biological Crystallography, 2010, 66, 1121-1123.	2.5	5
247	Coupling of receptor conformation and ligand orientation determine graded activity. Nature Chemical Biology, 2010, 6, 837-843.	8.0	121
248	Hitherto Unrecognized Fluorescence Properties of Coniferyl Alcohol. Molecules, 2010, 15, 1645-1667.	3.8	6
249	Crystal Structures of a Group II Chaperonin Reveal the Open and Closed States Associated with the Protein Folding Cycle. Journal of Biological Chemistry, 2010, 285, 27958-27966.	3.4	66
250	Evidence of Functional Protein Dynamics from X-Ray Crystallographic Ensembles. PLoS Computational Biology, 2010, 6, e1000911.	3.2	32
251	The PSI SGKB Technology Portal - An Online Database of Structural Genomics Technologies. Biophysical Journal, 2010, 98, 250a.	0.5	0
252	How to use the PSI Structural Genomics Knowledgebase to Enable Research. Biophysical Journal, 2010, 98, 250a.	0.5	0

#	Article	IF	CITATIONS
253	A Microscale Platform for Integrated Cell-Free Expression and Activity Screening of Cellulases. Journal of Proteome Research, 2010, 9, 5677-5683.	3.7	10
254	Microfluidic Glycosyl Hydrolase Screening for Biomass-to-Biofuel Conversion. Analytical Chemistry, 2010, 82, 9513-9520.	6.5	14
255	Photon Science at the ALS for Sustainable Energy. Synchrotron Radiation News, 2010, 23, 8-15.	0.8	Ο
256	Biochemical characterization and crystal structure of endoglucanase Cel5A from the hyperthermophilic Thermotoga maritima. Journal of Structural Biology, 2010, 172, 372-379.	2.8	65
257	Raman imaging of cell wall polymers in Arabidopsis thaliana. Biochemical and Biophysical Research Communications, 2010, 395, 521-523.	2.1	42
258	New tools for structure refinement in <i>PHENIX</i> . Acta Crystallographica Section A: Foundations and Advances, 2010, 66, s15-s15.	0.3	205
259	POLYGONand other tools: model validation at a glance. Acta Crystallographica Section A: Foundations and Advances, 2010, 66, s311-s312.	0.3	1
260	Spectroscopic Analyses of the Biofuels-Critical Phytochemical Coniferyl Alcohol and Its Enzyme-Catalyzed Oxidation Products. Molecules, 2009, 14, 4758-4778.	3.8	4
261	The protein structure initiative structural genomics knowledgebase. Nucleic Acids Research, 2009, 37, D365-D368.	14.5	94
262	Recent developments in phasing and structure refinement for macromolecular crystallography. Current Opinion in Structural Biology, 2009, 19, 566-572.	5.7	23
263	Label-free in situ imaging of lignification in the cell wall of low lignin transgenic Populus trichocarpa. Planta, 2009, 230, 589-597.	3.2	80
264	Crystallographic model quality at a glance. Acta Crystallographica Section D: Biological Crystallography, 2009, 65, 297-300.	2.5	95
265	Generalized X-ray and neutron crystallographic analysis: more accurate and complete structures for biological macromolecules. Acta Crystallographica Section D: Biological Crystallography, 2009, 65, 567-573.	2.5	137
266	Decision-making in structure solution using Bayesian estimates of map quality: the <i>PHENIX AutoSol</i> wizard. Acta Crystallographica Section D: Biological Crystallography, 2009, 65, 582-601.	2.5	804
267	Structure of endoglucanase Cel9A from the thermoacidophilic <i>Alicyclobacillus acidocaldarius</i> . Acta Crystallographica Section D: Biological Crystallography, 2009, 65, 744-750.	2.5	29
268	Averaged kick maps: less noise, more signal…and probably less bias. Acta Crystallographica Section D: Biological Crystallography, 2009, 65, 921-931.	2.5	59
269	<i>electronic Ligand Builder and Optimization Workbench</i> (<i>eLBOW</i>): a tool for ligand coordinate and restraint generation. Acta Crystallographica Section D: Biological Crystallography, 2009, 65, 1074-1080.	2.5	1,035
270	On the use of logarithmic scales for analysis of diffraction data. Acta Crystallographica Section D: Biological Crystallography, 2009, 65, 1283-1291.	2.5	18

#	Article	IF	CITATIONS
271	Automatic multiple-zone rigid-body refinement with a large convergence radius. Journal of Applied Crystallography, 2009, 42, 607-615.	4.5	49
272	A rapid and inexpensive labeling method for microarray gene expression analysis. BMC Biotechnology, 2009, 9, 97.	3.3	24
273	Transmembrane signal transduction of the αllbβ3 integrin. Protein Science, 2009, 11, 1800-1812.	7.6	78
274	Torsion Angle Refinement and Dynamics as a Tool to Aid Crystallographic Structure Determination. , 2009, , .		1
275	Iterative model building, structure refinement and density modification with the <i>PHENIX AutoBuild</i> wizard. Acta Crystallographica Section D: Biological Crystallography, 2008, 64, 61-69.	2.5	1,319
276	Surprises and pitfalls arising from (pseudo)symmetry. Acta Crystallographica Section D: Biological Crystallography, 2008, 64, 99-107.	2.5	81
277	Iterative-build OMIT maps: map improvement by iterative model building and refinement without model bias. Acta Crystallographica Section D: Biological Crystallography, 2008, 64, 515-524.	2.5	165
278	Protein structures by spallation neutron crystallography. Journal of Synchrotron Radiation, 2008, 15, 215-218.	2.4	35
279	<i>Web-Ice</i> : integrated data collection and analysis for macromolecular crystallography. Journal of Applied Crystallography, 2008, 41, 176-184.	4.5	81
280	Addressing the Need for Alternative Transportation Fuels: The Joint BioEnergy Institute. ACS Chemical Biology, 2008, 3, 17-20.	3.4	44
281	The development of an automated data analysis system for high-pressure powder diffraction data collected using an area detector. High Pressure Research, 2008, 28, 293-298.	1.2	2
282	Structural Genomics of Minimal Organisms: Pipeline and Results. Methods in Molecular Biology, 2008, 426, 475-496.	0.9	3
283	Macromolecular refinement at subatomic resolution with interatomic scatterers. Acta Crystallographica Section A: Foundations and Advances, 2008, 64, C22-C23.	0.3	1
284	Cctbx architecture and algorithms. Acta Crystallographica Section A: Foundations and Advances, 2008, 64, C44-C45.	0.3	0
285	The PSI structural genomics knowledgebase. Acta Crystallographica Section A: Foundations and Advances, 2008, 64, C364-C364.	0.3	0
286	SPARX, a new environment for Cryo-EM image processing. Journal of Structural Biology, 2007, 157, 47-55.	2.8	356
287	Technical Report: Recent Major Improvements to the ALS Sector 5 Macromolecular Crystallography Beamlines. Synchrotron Radiation News, 2007, 20, 23-30.	0.8	2
288	<i>Phaser</i> crystallographic software. Journal of Applied Crystallography, 2007, 40, 658-674.	4.5	17,782

#	Article	IF	CITATIONS
289	Ligand identification using electron-density map correlations. Acta Crystallographica Section D: Biological Crystallography, 2007, 63, 101-107.	2.5	57
290	Interpretation of ensembles created by multiple iterative rebuilding of macromolecular models. Acta Crystallographica Section D: Biological Crystallography, 2007, 63, 597-610.	2.5	60
291	On macromolecular refinement at subatomic resolution with interatomic scatterers. Acta Crystallographica Section D: Biological Crystallography, 2007, 63, 1194-1197.	2.5	59
292	Structure of O67745_AQUAE, a hypothetical protein fromAquifex aeolicus. Acta Crystallographica Section F: Structural Biology Communications, 2007, 63, 369-374.	0.7	7
293	Phenix refine developments. Acta Crystallographica Section A: Foundations and Advances, 2007, 63, s80-s80.	0.3	0
294	Automated ligand fitting by core-fragment fitting and extension into density. Acta Crystallographica Section D: Biological Crystallography, 2006, 62, 915-922.	2.5	98
295	Improved statistics for determining the Patterson symmetry from unmerged diffraction intensities. Journal of Applied Crystallography, 2006, 39, 158-168.	4.5	20
296	Structural Basis for Double-Stranded RNA Processing by Dicer. Science, 2006, 311, 195-198.	12.6	860
297	Crystal structures of a phosphotransacetylase from Bacillus subtilis and its complex with acetyl phosphate. Journal of Structural and Functional Genomics, 2006, 6, 269-279.	1.2	20
298	Automated structure determination with PHENIX. Acta Crystallographica Section A: Foundations and Advances, 2006, 62, s85-s85.	0.3	2
299	Structural Genomics of Minimal Organisms and Protein Fold Space. Journal of Structural and Functional Genomics, 2005, 6, 63-70.	1.2	29
300	A robust bulk-solvent correction and anisotropic scaling procedure. Acta Crystallographica Section D: Biological Crystallography, 2005, 61, 850-855.	2.5	153
301	Automated crystallographic ligand building using the medial axis transform of an electron-density isosurface. Acta Crystallographica Section D: Biological Crystallography, 2005, 61, 1354-1363.	2.5	13
302	FINDMOL: automated identification of macromolecules in electron-density maps. Acta Crystallographica Section D: Biological Crystallography, 2005, 61, 1514-1520.	2.5	3
303	Structure of a NAD kinase fromThermotoga maritimaat 2.3â€Ã resolution. Acta Crystallographica Section F: Structural Biology Communications, 2005, 61, 640-646.	0.7	10
304	Crystal structure of DNA sequence specificity subunit of a type I restriction-modification enzyme and its functional implications. Proceedings of the National Academy of Sciences of the United States of America, 2005, 102, 3248-3253.	7.1	66
305	Crystal Structure of a PhoU Protein Homologue. Journal of Biological Chemistry, 2005, 280, 15960-15966.	3.4	33
306	Crystal Structure of the "PhoU-Like―Phosphate Uptake Regulator from Aquifex aeolicus. Journal of Bacteriology, 2005, 187, 4238-4244.	2.2	29

#	Article	IF	CITATIONS
307	Crystal structure of a bacterial ribonuclease P RNA. Proceedings of the National Academy of Sciences of the United States of America, 2005, 102, 13392-13397.	7.1	206
308	Crystal Structure of a Heat-inducible Transcriptional Repressor HrcA from Thermotoga maritima: Structural Insight into DNA Binding and Dimerization. Journal of Molecular Biology, 2005, 350, 987-996.	4.2	24
309	Crystal Structures of an NAD Kinase from Archaeoglobus fulgidus in Complex with ATP, NAD, or NADP. Journal of Molecular Biology, 2005, 354, 289-303.	4.2	35
310	Computational Aspects of High-Throughput Crystallographic Macromolecular Structure Determination. Methods of Biochemical Analysis, 2005, 44, 75-87.	0.2	0
311	A robust bulk solvent correction and anisotropic scaling procedure in the CCTBX. Acta Crystallographica Section A: Foundations and Advances, 2005, 61, c160-c160.	0.3	4
312	Hybrid programming in crystallography: Phenix.refine and Phenix.hyss. Acta Crystallographica Section A: Foundations and Advances, 2005, 61, c81-c82.	0.3	0
313	mmCIF and modern macromolecular structure determination software: status and perspectives. Acta Crystallographica Section A: Foundations and Advances, 2005, 61, c127-c127.	0.3	0
314	Recent developments in thePHENIXsoftware for automated crystallographic structure determination. Journal of Synchrotron Radiation, 2004, 11, 53-55.	2.4	319
315	Numerically stable algorithms for the computation of reduced unit cells. Acta Crystallographica Section A: Foundations and Advances, 2004, 60, 1-6.	0.3	47
316	Robust indexing for automatic data collection. Journal of Applied Crystallography, 2004, 37, 399-409.	4.5	149
317	Structural basis of light chain amyloidogenicity: comparison of the thermodynamic properties, fibrillogenic potential and tertiary structural features of four Vλ6 proteins. Journal of Molecular Recognition, 2004, 17, 323-331.	2.1	73
318	Crystal Structures of the Rhodococcus Proteasome with and without its Pro-peptides: Implications for the Role of the Pro-peptide in Proteasome Assembly. Journal of Molecular Biology, 2004, 335, 233-245.	4.2	80
319	Exploring the Structural Dynamics of the E.coli Chaperonin GroEL Using Translation-libration-screw Crystallographic Refinement of Intermediate States. Journal of Molecular Biology, 2004, 342, 229-245.	4.2	109
320	Role of the Â-phosphate of ATP in triggering protein folding by GroEL-GroES: function, structure and energetics. EMBO Journal, 2003, 22, 4877-4887.	7.8	130
321	X-Ray Crystallographic and Kinetic Studies of Human Sorbitol Dehydrogenase. Structure, 2003, 11, 1071-1085.	3.3	83
322	Substructure search procedures for macromolecular structures. Acta Crystallographica Section D: Biological Crystallography, 2003, 59, 1966-1973.	2.5	214
323	On symmetries of substructures. Acta Crystallographica Section D: Biological Crystallography, 2003, 59, 1974-1977.	2.5	8
324	High-resolution structure of RNase P protein from Thermotoga maritima. Proceedings of the National Academy of Sciences of the United States of America, 2003, 100, 7497-7502.	7.1	87

#	Article	IF	CITATIONS
325	Automatic Solution of Heavy-Atom Substructures. Methods in Enzymology, 2003, 374, 37-83.	1.0	34
326	Molecular Dynamics Applied to X-ray Structure Refinement. Accounts of Chemical Research, 2002, 35, 404-412.	15.6	68
327	TheComputational Crystallography Toolbox: crystallographic algorithms in a reusable software framework. Journal of Applied Crystallography, 2002, 35, 126-136.	4.5	262
328	On the handling of atomic anisotropic displacement parameters. Journal of Applied Crystallography, 2002, 35, 477-480.	4.5	48
329	Algorithms for deriving crystallographic space-group information. II. Treatment of special positions. Acta Crystallographica Section A: Foundations and Advances, 2002, 58, 60-65.	0.3	24
330	PHENIX: building new software for automated crystallographic structure determination. Acta Crystallographica Section D: Biological Crystallography, 2002, 58, 1948-1954.	2.5	3,979
331	Patterson correlation methods: a review of molecular replacement withCNS. Acta Crystallographica Section D: Biological Crystallography, 2001, 57, 1390-1396.	2.5	11
332	Recent developments in software for the automation of crystallographic macromolecular structure determination. Current Opinion in Structural Biology, 2000, 10, 564-568.	5.7	16
333	Use of a New Label, 13Cî—»18O, in the Determination of a Structural Model of Phospholamban in a Lipid Bilayer. Spatial Restraints Resolve the Ambiguity Arising from Interpretations of Mutagenesis Data. Journal of Molecular Biology, 2000, 300, 677-685.	4.2	92
334	Extending the limits of molecular replacement through combined simulated annealing and maximum-likelihood refinement. Acta Crystallographica Section D: Biological Crystallography, 1999, 55, 181-190.	2.5	30
335	Annealing in crystallography: a powerful optimization tool. Progress in Biophysics and Molecular Biology, 1999, 72, 135-155.	2.9	25
336	Experimentally based orientational refinement of membrane protein models: a structure for the Influenza A M2 H + channel 1 1Edited by G. von Heijne. Journal of Molecular Biology, 1999, 286, 951-962.	4.2	141
337	Models for the Transmembrane Region of the Phospholamban Pentamer: Which Is Correct? a. Annals of the New York Academy of Sciences, 1998, 853, 178-185.	3.8	9
338	Crystallography & NMR System: A New Software Suite for Macromolecular Structure Determination. Acta Crystallographica Section D: Biological Crystallography, 1998, 54, 905-921.	2.5	14,711
339	Recent developments for the efficient crystallographic refinement of macromolecular structures. Current Opinion in Structural Biology, 1998, 8, 606-611.	5.7	83
340	New Applications of Simulated Annealing in Crystallographic Refinement. , 1998, , 143-157.		2
341	STRUCTURAL PERSPECTIVES OF PHOSPHOLAMBAN, A HELICAL TRANSMEMBRANE PENTAMER. Annual Review of Biophysics and Biomolecular Structure, 1997, 26, 157-179.	18.3	67
342	Cross-validated maximum likelihood enhances crystallographic simulated annealing refinement. Proceedings of the National Academy of Sciences of the United States of America, 1997, 94, 5018-5023.	7.1	623

#	Article	IF	CITATIONS
343	New applications of simulated annealing in X-ray crystallography and solution NMR. Structure, 1997, 5, 325-336.	3.3	197
344	Structure of the Transmembrane Cysteine Residues in Phospholamban. Journal of Membrane Biology, 1997, 155, 199-206.	2.1	25
345	Improved prediction for the structure of the dimeric transmembrane domain of glycophorin A obtained through global searching. Proteins: Structure, Function and Bioinformatics, 1996, 26, 257-261.	2.6	149
346	Improved prediction for the structure of the dimeric transmembrane domain of glycophorin A obtained through global searching. Proteins: Structure, Function and Bioinformatics, 1996, 26, 257-261.	2.6	6
347	Computational searching and mutagenesis suggest a structure for the pentameric transmembrane domain of phospholamban. Nature Structural and Molecular Biology, 1995, 2, 154-162.	8.2	198
348	Conformational variability in the refined structure of the chaperonin GroEL at 2.8 Ã resolution. Nature Structural and Molecular Biology, 1995, 2, 1083-1094.	8.2	219
349	Structural organization of the pentameric transmembrane alpha-helices of phospholamban, a cardiac ion channel EMBO Journal, 1994, 13, 4757-4764.	7.8	175
350	A dimerization motif for transmembrane α–helices. Nature Structural Biology, 1994, 1, 157-163.	9.7	294
351	Structure of rodent urinary proteins. Biochemical Society Transactions, 1990, 18, 936-937.	3.4	11